

Figure 3.1
Sketch of wing-body showing forces, moments and distances.



Figure 3.2

The Indian Light Combat Aircraft (LCA)—a tailless wing–body configuration. (<http://www.defenceforumindia.com>; http://3.bp.blogspot.com/_2istSpJf6tk/TOTT-xyHRLI/AAAAAAAAApE/way1ML29vsA/s1600/lca-tejas-9.jpg)

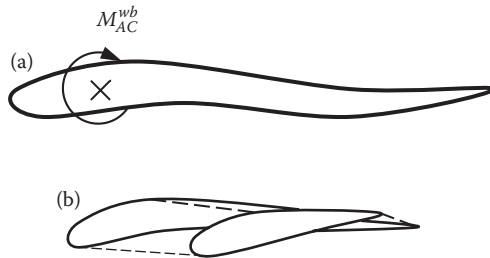


Figure 3.3

(a) An airfoil with reflex camber at the trailing edge and (b) a wing sweep and twist arrangement.

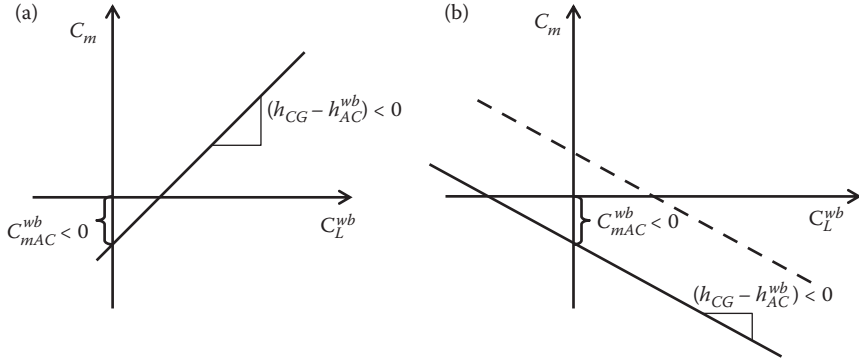


Figure 3.4

Graphs of C_m plotted against C_L^{wb} for two cases: (a) CG behind AC^{wb} and (b) CG ahead of AC^{wb} .

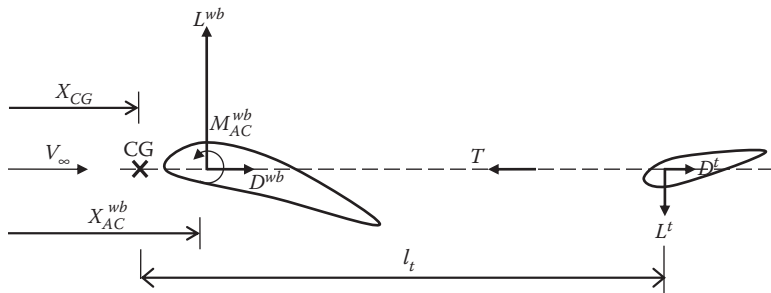


Figure 3.5
Schematic representation of the wing-body plus tail trim and stability.

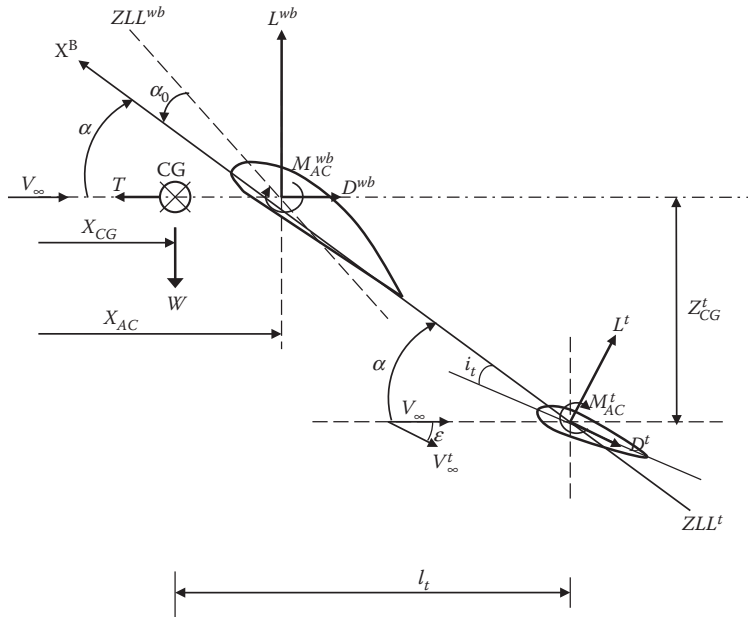


Figure 3.6
Wing-body and horizontal tail configuration.

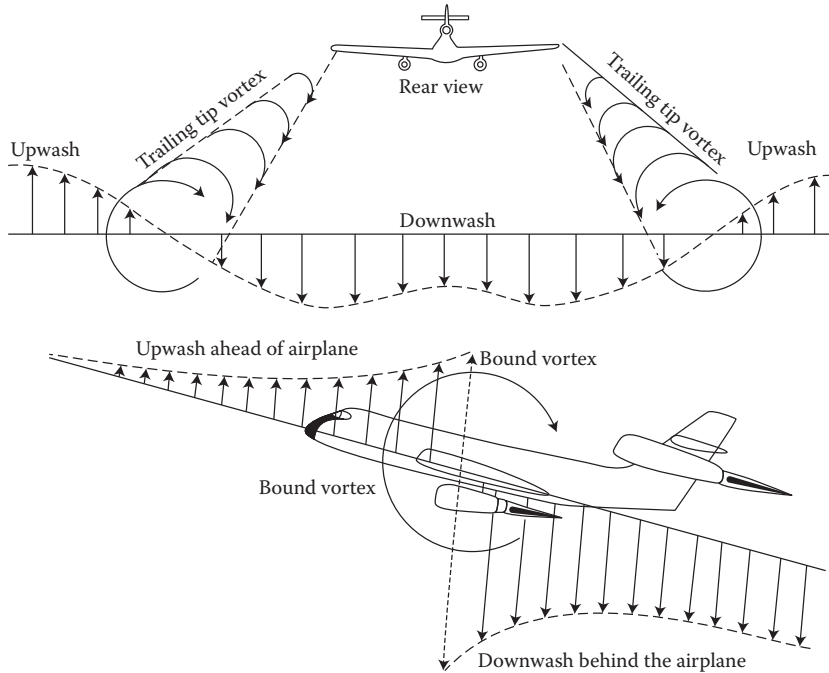


Figure 3.7

Upwash and downwash due to flowfield around wing. (With permission from Gustavo Corujo, <http://history.nasa.gov>; <http://history.nasa.gov/SP-367/f54.htm>)



Figure 3.8

Trailing edge vortices emanating from tips of the wing of an airplane seen in the clouds. (http://flyingindian.files.wordpress.com/2010/09/wingtip_vortices_lg.jpg)



Figure 3.9

Example of a T-tail configuration. (www.airliners.net) (<http://origin-www.airliners.net/aviation-photos/small/4/1/1/1972114.jpg>)

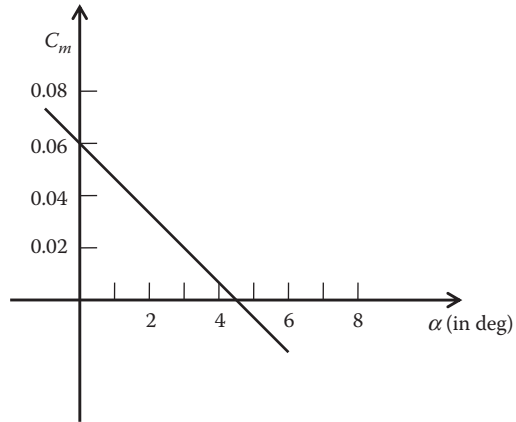


Figure 3.10
Plot of C_m versus α in Example 3.5.

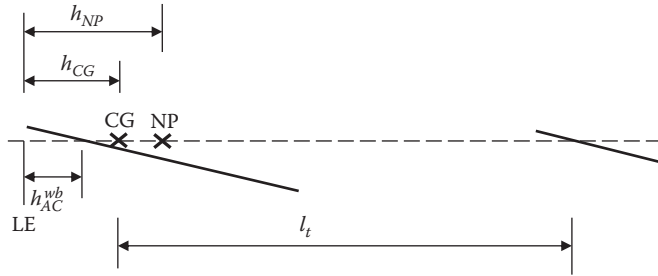


Figure 3.11
Sketch for Example 3.6 ($h_{CG} \sim 0.36$ and $h_{NP} \sim 0.526$).

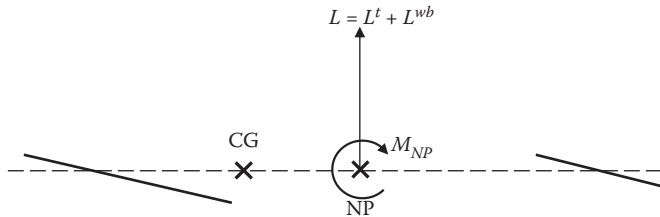


Figure 3.12

Sketch of forces and moment on an airplane displayed at the neutral point.

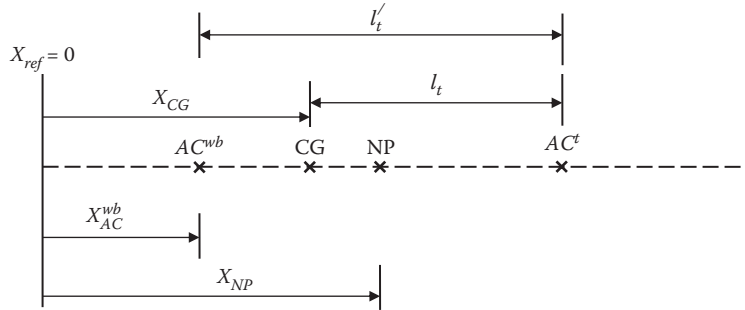


Figure 3.13

Sketch of various locations and distances in case of a wing-body-plus tail.

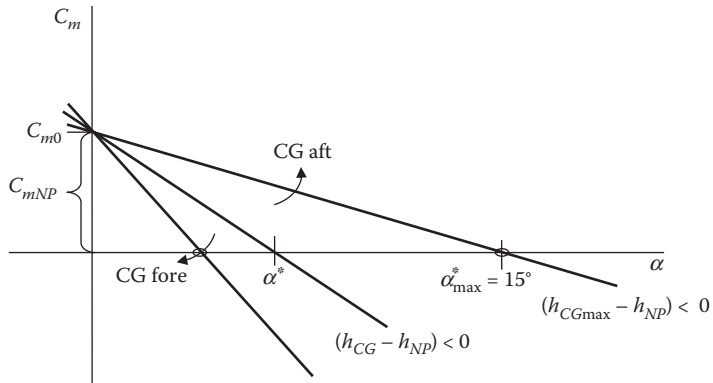


Figure 3.14

Graph of C_m versus α showing the effect of shift in CG position, and the practical rearmost CG position corresponding to trim at landing angle of attack, here taken to be nominally 15° . (http://www.aerospace-web.org/aircraft/jetliner/b747/b747_21.jpg)

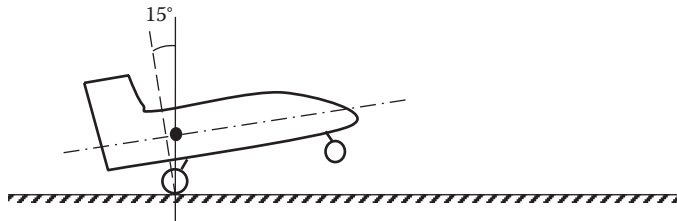


Figure 3.15

Sketch of airplane and rearmost allowable *CG* position during rotation at take-off ground run.



Figure 3.16

Example of a ‘tail-sitting’ airplane due to improper loads on the ground. (http://www.aerospaceweb.org/aircraft/jetliner/b747/b747_21.jpg)

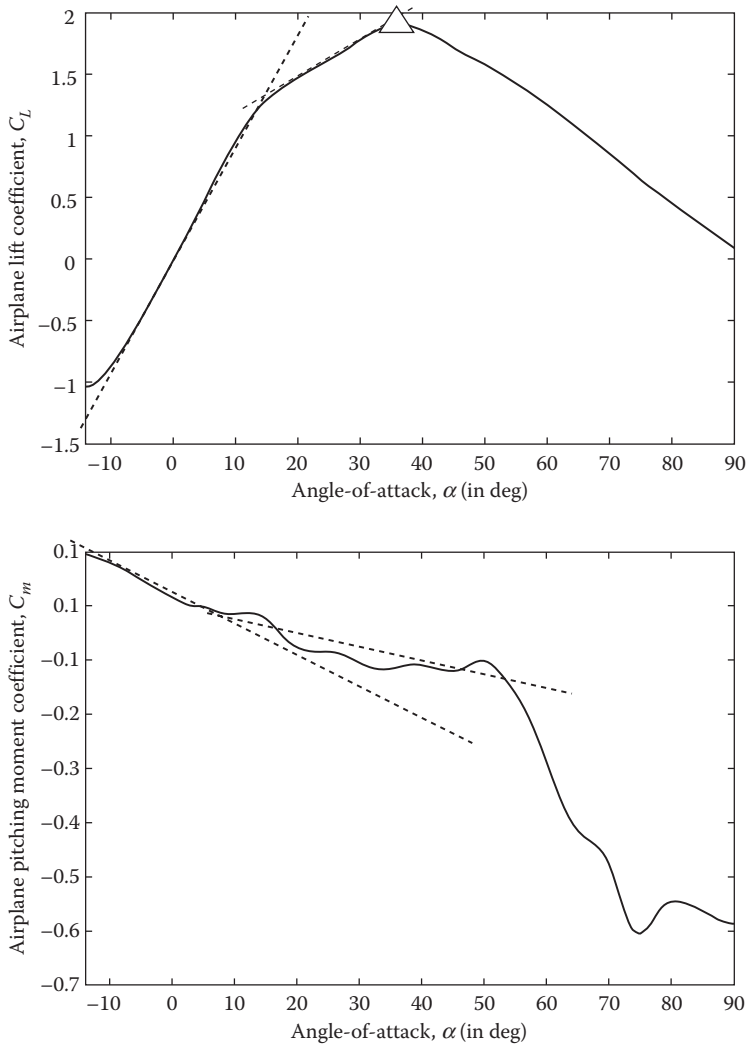


Figure 3.17
Variation of C_L and C_m for the F-18/HARV from -14° to $+90^\circ$ angle of attack (\boxtimes -Stall).

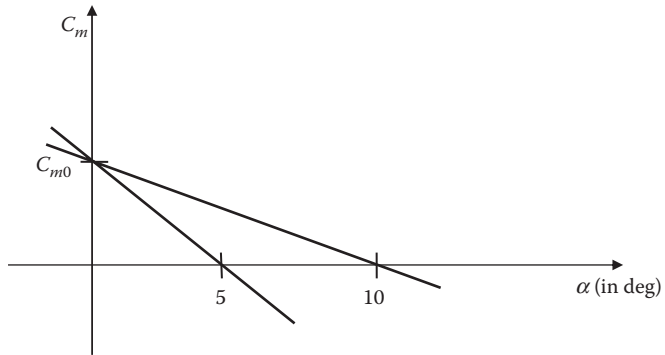


Figure 3.18

C_m versus α curve of a general aviation airplane.

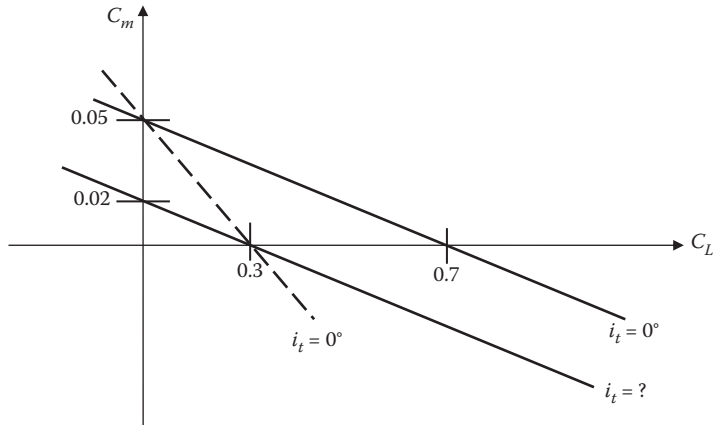


Figure 3.19
 C_m - C_L curve for an airplane for different tail setting angles.

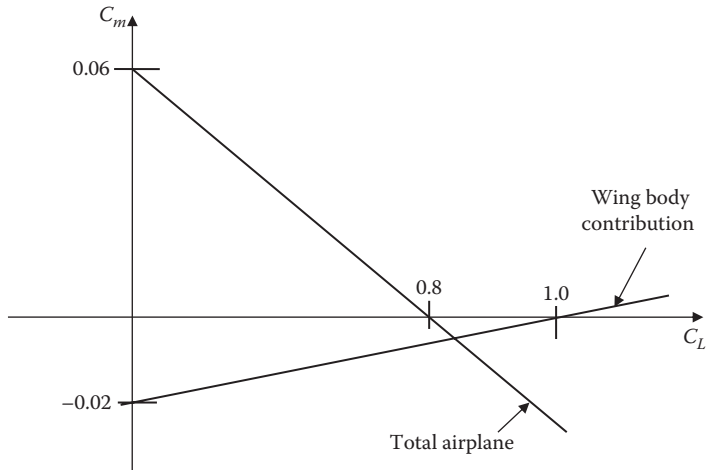


Figure 3.20

C_m - α curve for an airplane with contributions from individual components.

Courtesy of CRC Press/Taylor & Francis Group



(Source: <http://alain.vassel.pages-perso-orange.fr/siecle19.htm>)

ITX003X001.tif

Courtesy of CRC Press/Taylor & Francis Group



(Source: <http://commons.wikimedia.org/File:AlphonsePenaudPlenophore.jpg>)

ITX003X002.tif